PCCP

Accepted Manuscript

ROYAL SOCIETY OF CHEMISTRY

www.rsc.org/pccp

PCCP

RSCPublishing

ARTICLE

Temperature sensing from the emission rise times of Eu^{3+} in SrY_2O_4

Cite this: DOI: 10.1039/x0xx00000x

V. Lojpur, Ž. Antić and M. D. Dramićanin*

Received 00th January 2012,
Accepted 00th January 2012

DOI: 10.1039/x0xx00000x

www.rsc.org/

The emission rise time of Eu^{3+}-doped SrY_2O_4 was investigated in the temperature range of 20–200 °C for application in luminescent thermometry. After pulsed excitation, the energy transfer between adjacent Eu^{3+} ions causes a emission build-up from the $^5D_0$ level of Eu^{3+} and a notable emission rise occurs prior to decay. The emission rise-time values linearly decrease with temperature, providing absolute sensitivity of 0.66 μs°C^{-1} and maximal relative sensitivity of 5.53 %°C^{-1} at 200 °C, for samples containing 0.5 at.% Eu^{3+} ions. It is shown that the time after excitation at which emission reaches maximum (time-to-max) can also be exploited for temperature sensing, since it is easily measurable and shows a linear dependence with temperature.

Introduction

The accurate and reliable measurement of temperature is essential in many fields: in industry, agriculture, military, science, etc. Consequently, temperature is by far the most-measured physical quantity, and temperature sensors account for ~75–80% of the world's sensor market.[1-3] Today, temperature is usually measured using liquid-filled glass thermometers, thermocouples, and infrared optical devices. In recent times, novel temperature measurement concepts have emerged,[4-6] especially for non-contact measurements, measurements in harsh environments or at points which are difficult to access, and measurements with nanoscale spatial resolution. Among these concepts, non-contact luminescence thermometry has garnered the most attention.[1,7-9]

With various types of luminescent materials, temperature evolution can be remotely measured according to changes in the material's luminescent properties, including emission intensities, spectral-band shapes, temporal behaviours of emission, and anisotropy.[10-18] Among different modalities of luminescence thermometry, temperature evaluations through relative emission intensity measurements (ratiometric intensity measurements) and through measurements of temporal changes of emission (emission decay times and rise times) are of particular importance, as they are self-referencing (i.e., these types of measurements do not have to refer to any temperature standard). These two methods exhibit some comparative advantages and disadvantages. Ratiometric intensity measurements are faster and generally require less-sophisticated equipment than measurements of temporal dependence of emission. The latter method, on the other hand, is not affected by light scattering, reflection, or inhomogeneous distribution of the sensing material, all of which may compromise ratiometric intensity methods. Also, thermometry by measurement of temporal emission behaviour only requires monitoring a single emission, while ratiometric intensity measurement needs two emission bands, which is not always feasible. However, the critical difference between these methods is that ratiometric intensity methods generally have larger dynamic ranges and higher relative sensitivities than emission decay methods.[1,7,8,19,20] In addition, in many materials tested for luminescent thermometry emission decay constants (lifetimes) have minor or negligible temperature dependence in the vicinity of room temperature, which is a critical range for the majority of applications. As a result, ratiometric intensity methods have been used in many more applications in the past than those based on emission decay.

Ranson *et al.*[21] and Allison *et al.*[22] have shown that luminescence thermometry based on measurements of emission rise times have better sensitivities and more suitable sensing ranges than thermometry based on emission decay times. A rise in emission intensity can be observed during the period prior to emission decay as a consequence of fast non-radiative relaxations from excited states of higher energy and/or energy transfer (ET) from surroundings. Ranson *et al.*[21] and Allison *et al.*[22] have investigated the rise time of emission from the $^5D_0$ level of Eu^{3+} incorporated in Y_2O_3 by monitoring 611-nm emission ($^5D_0 \rightarrow {}^7F_2$ transition). Considering that trivalent europium ions (and other trivalent rare-earth ions) substitute with Y^{3+} at two different crystallographic sites, C_2 and C_{3i} (S_6), in Y_2O_3, they concluded that the initial emission increase at 611 nm is a consequence of ET into the $^5D_0$ level of Eu^{3+} in the C_2 sites from the $^5D_1$ energy levels of Eu^{3+} in the C_2 and C_{3i} sites, and from ET from the $^5D_0$ level of Eu^{3+} in the C_{3i} sites. This conclusion was in agreement with a previous report by Herber *et al.*[23] Ranson *et al.*[21] also concluded that the main contribution to the initial emission rise is caused by ET from the $^5D_1$ level of Eu^{3+} in the C_{3i} sites to the $^5D_0$ level of Eu^{3+} in the C_2 sites, because it is appreciably slower than other ET's, owing to the centrosymmetric nature of the C_{3i} site, which was also in accordance with an earlier report from Herber *et al.*[23] Furthermore, by finding the temperature dependence of

emission rise time in Y_2O_3 doped with 0.5 at.% Eu^{3+}, Allison *et al.*[22] measured temperatures from ambient to 700 °C. Over this range, the emission rise time value decreases from ~110 μs to ~9 μs, which corresponds to an absolute sensitivity of 0.148 $\mu s°C^{-1}$.

However, since these first promising reports were published, no work has been reported on the use of emission rise times for luminescence thermometry. There are three probable reasons for this course of events: The rise of emission occurs in the initial period after the excitation pulse, prior to emission decay, and in routine measurements this period is often considered as ''dead time'', and is therefore frequently ignored in the analysis of emission. Secondly, rise times are notably shorter than decay times, and they are further reduced with increasing temperature. In addition, similarly to decay times, rise times undergo concentration quenching. Thirdly, concentrations of luminescent centres in luminescent materials are optimized for efficient emission, and these concentrations can be too high for observing emission rise times suitable for temperature sensing.

In this work, we aimed to find suitable materials for luminescence thermometry based on the temperature dependence of emission rise time that are capable of sensing near room temperature. We hypothesized that rare-earth-doped phosphor may be appropriate, because phosphor materials have long-lived excited states and intense emissions. The host material for the incorporation of rare-earth ions should have two or more different crystallographic sites to facilitate efficient emission build-up, where the short distance between sites facilitates efficient energy transfer between ions. Long rise and decay times can then be achieved with a low concentration of rare-earth ion activators.

The aforementioned conditions can be met with ARe_2O_4 (A = Ca, Sr, Ba; Re = Y, Gd, Lu, Sc, In), a type of oxide material that has been recently proposed as promising host for the preparation of rare-earth based phosphors.[24] Herein, we analysed Eu^{3+} doped SrY_2O_4, which has been described[25] as a novel red-emitting phosphor for fluorescent lamps and field emission displays with a superior colour rendering index compared to conventional red phosphors.

Experimental

For this investigation, powders of SrY_2O_4 doped Eu^{3+} were obtained by the citrate sol-gel method after thermal treatment in air at 1000 °C for 2h. The detailed synthesis procedure is given in the Ref. 26. In brief, SrY_2O_4 samples doped with different concentrations of Eu^{3+} (0.25, 0.5, 1.5, 3, and 5 at.%) were prepared *via* citrate sol-gel method using glycine as a fuel. Firstly, yttrium nitrate hexahidrate, $(Y(NO_3)_3{\cdot}6H_2O$, and europium nitrate hexahidrate, $(Eu(NO_3)_3{\cdot}6H_2O$, were dissolved in deionized water, while strontium nitrate, $Sr(NO_3)_2$, was dissolved in deionized water separately. Then, citric acid $[HOC(COOH)(CH_2COOH)_2]$ was added to both solutions and left for dissolving for a 1.5 h on a hot plate with continued magnetic stirring at 60 °C. Then the solutions were joined, glycine $[NH_2CH_2COOH]$ was added to the solution, and temperature was raised to 120 °C. After approximately 1 h wet gel was produced and subsequently burned in the furnace at 500 °C for 1.5 h. Finally, the sample was calcinated for 2 h at 1000 °C.

Photoluminescence measurements were performed at room temperature using a Fluorolog-3 spectrofluorometer (FL3-221, Horiba Jobin Yvon), which uses a 450-W xenon lamp as an excitation source for steady-state emission measurements and a xenon–mercury pulsed lamp for time-resolved emission measurements. The signal was detected with a fast TBX-04 detector. The emission spectrum was scanned for the wavelength range 560–750 nm under 393-nm excitation radiation (in the $^5L_6$ Eu^{3+} level). Temporal emission behaviour was recorded while maintaining powders at various temperatures ranging from 20 to 200 °C in a custom-made furnace. Powder morphology was evaluated by scanning electron microscopy (SEM) using JEOL JSM-6610LV instrument (at operating voltage of 20 kV). X-ray diffraction measurements were performed using a Rigaku SmartLab diffractometer. Diffraction data were recorded in the 2θ range from 10º to 90º, at a counting speed of 0.7º/min in 0.02º steps.

Results and discussion

SEM analysis of Eu^{3+} doped SrY_2O_4 samples revealed powders composed of agglomerated spherical-like particles with good packing density, and particle diameter of about 200 nm, as shown in the Figure 1.

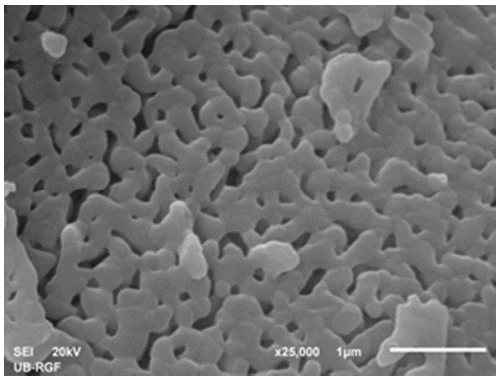

Fig. 1 SEM micrograph of SrY_2O_4 doped with 0.5 at.% of Eu^{3+} obtained with ×25.000 magnification.

An X-ray diffraction pattern for Eu^{3+} doped SrY_2O_4 is shown in Figure 2. The main reflections were indexed according to the JCPDS 32-1272 card, and no reflections from impurity phases were detected.

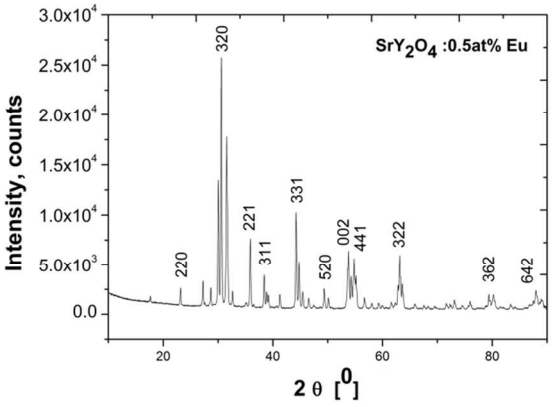

Fig. 2 X-ray diffraction pattern for SrY_2O_4 sample doped with 0.5 at. % Eu^{3+} indexed according to the JCPDS 32-1272 card

SrY_2O_4 crystallizes in the orthogonal $CaFe_2O_4$ structure with the *Pnam* space group. Its structure has two different sites for Y^{3+} ions. One of them (Y_1) is nearly octahedral while the other (Y_2) possess a more disordered coordination environment (see Figure 3). In both sites, Y^{3+} ions are coordinated by six oxygen atoms, and both sites have Cs symmetry.[27-30] The orthorhombic structure is composed of a double-octahedral $Y_2O_4^{2-}$ framework with embedded Sr^{2+} ions.[27]

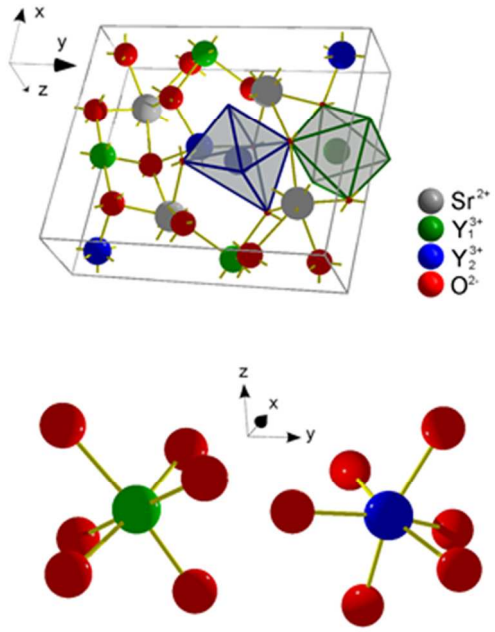

Fig. 3 Schematic representation of the SrY_2O_4 crystal structure, along with the coordination environment of its Y_1 and Y_2 sites.

A photoluminescence emission spectra for Eu^{3+} (0.5 at.%) doped SrY_2O_4 measured at different temperatures in the range from 20-200°C are presented in Figure 4(a). The spectra are composed of sharp emissions from the $^5D_0 \rightarrow {}^7F_J$ (J = 0, 1, 2, 3, 4) electron transitions of Eu^{3+} ions located in both crystallographic sites. The increase in temperature cause emission quenching. In the range from 20 to 200°C emission intensity is reduced by a factor of two. Even though emission intensity shows significant temperature dependence, luminescence sensing of temperatures based on measurements of the intensity of emission from a single excited state depend crucially on optoelectronic drifts of the excitation source and detectors, rendering them incapable of producing accurate thermometric measurements.[17] Conversely, ratiometric intensity measurements and emission temporal dependences are not compromised by these disadvantages and, consequently, are much more reliable. For ratiometric intensity temperature sensing with Eu^{3+} emissions one needs to record emissions from $^5D_0$ and $^5D_1$ levels. In the present case the $^5D_1$ emission located around 535 nm (Figure 4(a)) has very small intensity for use in reliable temperature sensing. Figure 4(b) shows room-temperature emission from the $^5D_0 \rightarrow {}^7F_0$ transition, recorded in the 578–583.5 nm range, with longer signal accumulation than in Figure 4(a). This transition is not split by the crystal field (since $J = 0$), so the number of observed emission lines corresponds to the number of different crystallographic sites (environments) in which Eu^{3+} ions are located. Two distinct peaks at 580.8 and 582.1 nm confirm the two distinctive crystallographic environments for Eu^{3+} ions. One can assume that Eu^{3+} ions substitute with Y^{3+} in both sites (Y_1 and Y_2). This assumption is made on the basis of previous reports[27,28] related to the preferential occupation of rare-earth dopant ions in SrY_2O_4.

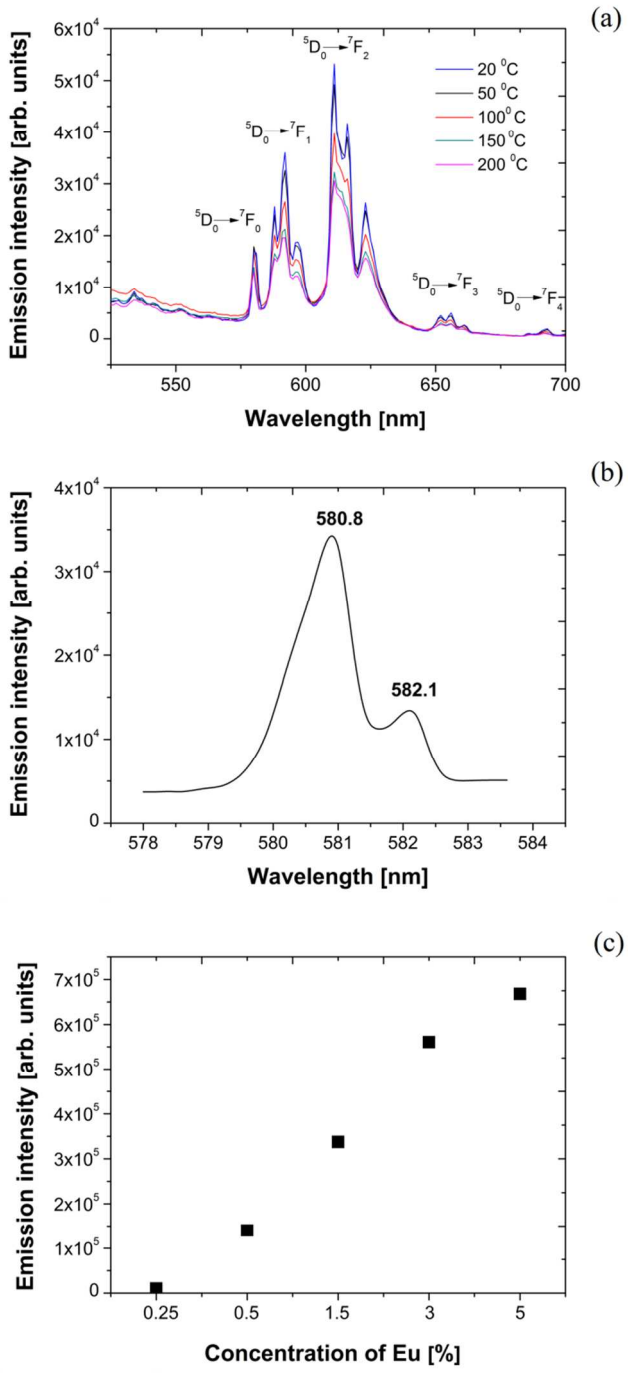

Fig. 4 (a) Photoluminescence emission spectra of SrY_2O_4 doped with 0.5 at.% Eu^{3+}; measured at different temperatures in the range from 20-200°C; (b) the splitting of the $^5D_0 \rightarrow {}^7F_0$ transition; (c) the Eu^{3+} concentration dependence of the 611 nm-emission intensity.

Moreover, according to these reports, the more intense emission at 611 nm than at 616.5 nm may be indicative of Eu^{3+} occupation slightly favouring the Y_1 site. Taking into account the difference in ionic radii of Eu^{3+} and Sr^{2+}, the relatively low doping concentration, and the low temperature used for powder preparation, Eu^{3+} occupation of Sr^{2+} sites has a low probability.[27,28] Figure 4(c) shows Eu^{3+} concentration dependence of the 611 nm-emission intensity. It is worth of noting that emission intensity rapidly increase with concentration until concentration of 3 at.% and fairly between 3 and 5 at.%.

Temporal behaviour of Eu^{3+} emission was monitored at 611 nm under pulsed excitation in the $^5L_6$ level of Eu^{3+} (393 nm). Owing to the overlap of Eu^{3+} emissions from the two crystallographic sites, the emission decay was expected to exhibit a double exponential behaviour. Two assumptions are made to describe the emission rise in a simple way. First, the $^5D_0$ level should be populated from levels of higher energy of the same ion much more rapidly (instantaneously) than by transitions from neighbouring ions.[21,31] Secondly, the latter process of emitting-level population is characterized by the decay constant τ_r, whose value does not differ depending on the direction of the transition (i.e., from ions in site 1 to ions in site 2 or vice versa). Then, according to Ranson *et al.*[21], the number of electrons in the emitting level, N, can be described as:

$$N = N_0 + N_1\left[1 - \exp(-\frac{t}{\tau_r})\right], \quad (1)$$

where N_0 stands for the population directly excited within the ion, and N_1 stands for the population obtained by the transition from neighbouring ions. The temporal dependence of emission intensity, $I(t)$, can be described by (taking into account that $I \propto N$):

$$I(t) = \left\{A + B\left[1 - \exp(-\frac{t}{\tau_r})\right]\right\}\left[\exp\left(-\frac{t}{\tau_{d1}}\right)\exp(-\frac{t}{\tau_{d2}})\right], \quad (2)$$

where τ_{d1} and τ_{d2} are the decay constants of emission from two crystallographic sites (lifetimes), and τ_r is the rise time constant; A and B are intensity parameters. An example of experimental data fitting by Eq. (2) is given in Figure 5. Here, the temporal dependence of emission intensity for SrY_2O_4 activated with 0.5 at.% Eu^{3+} is presented as open circles, with theoretical dependence as a solid line. This fitting procedure provided a rise-time value of τ_r = 138 μs, and decay-time values of τ_{d1} = 3882 μs and τ_{d2} = 1363 μs.

Table 1 summarizes the rise time and decay time values obtained for SrY_2O_4 with different concentrations of Eu^{3+}. The largest value (163 μs) is found for the lowest Eu^{3+} doping level of 0.25 at.%, and the value steadily decreases with increasing concentration. For further investigation of the temperature dependence of emission rise time, a doping level of 0.5 at.% was chosen, since 0.25 at.% Eu^{3+} emission may be too weak for practical application (see Figure 4(c)). One should note that decay times have a nearly constant value up to concentrations of 3 at.%, i.e., that concentration quenching of emission becomes apparent at Eu^{3+} concentrations higher than 3 at.%.

Table 1. Values of emission rise times and decay times in SrY_2O_4 for different Eu^{3+} doping concentrations.

Eu^{3+} (at.%)	0.25	0.5	1.5	3	5
τ_r (μs)	163±8	138±8	87±6	67±5	45±5
τ_{d1} (μs)	3906±22	3882±24	3511±20	3341±22	2164±21
τ_{d2} (μs)	1380±21	1363±22	1274±26	1264±22	828±17

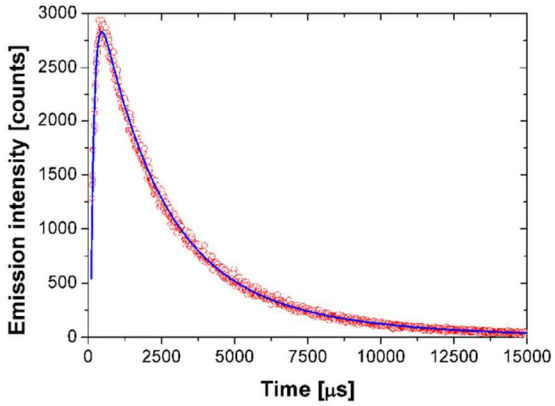

Fig. 5 Room-temperature rise and decay component of SrY_2O_4: 0.5 at.% Eu^{3+}; experimental data are shown as open circles, and the theoretical curve according to Eq. (2) is shown as a solid line.

Figure 6(a) presents temporal dependencies of emissions measured in the temperature range 20–200°C (some dependencies are omitted for image clarity).

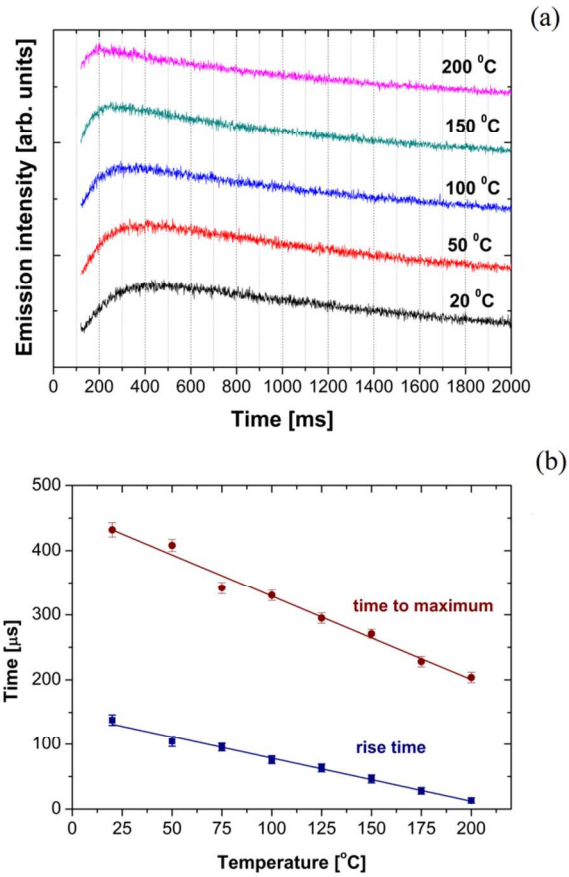

Fig. 6 (a) Temporal behaviour of the emission of SrY_2O_4 activated with 0.5 at.% Eu^{3+} recorded at different temperatures in the 20-200°C range; (b) temperature dependence of the rise time and time-to-max: experimental (symbols) and linear regression (lines).

Over this temperature range, the rise-time values linearly decrease by more than an order of magnitude [see Figure 6(b)],

$$\tau_r(T)|_{20°C}^{200°C} = 144.99\ (\pm 3.21) - 0.66\ (\pm 0.03) \times T[°C]. \quad (3)$$

Khalid and Kontis[32] showed that the analysis of the temporal behaviour of emission can be simplified by observing the time at which emission reaches a maximal value (time to maximum, t_m). Unlike rise-time value, which needs to be derived from the fitting procedure, time-to-max can be detected directly from experimental data, and this can be particularly important for rapid 2D-surface thermal imaging.[32] In the present case, the time-to-max value dependence on temperature is presented in Figure 6(b). Linear regression of the experimental data provided the following relation:

$$t_m(T)|_{20°C}^{200°C} = 457.56\ (\pm 8.06) - 1.29\ (\pm 0.06) \times T[°C]. \quad (4)$$

Even though linear dependence of a sensor parameter is not crucial for application, this attribute is always helpful. Measurements were repeated several times (several cycles with increasing and decreasing of temperature) and only fair variations in emission temporal behaviour were observed. Additionally, both parameters, rise time and time-to-max, had large changes in magnitudes with temperature increase, which can be easily observed in Figure 6(b). Such changes may suggest strong sensitivity of temperature measurement. Useful parameters for describing the performance of a temperature sensor are the absolute sensitivity (S_a) and the relative sensitivity (S_r), given by the following equations:

$$S_a = \left|\frac{\partial Q}{\partial T}\right| \text{ in } [\mu s/°C],$$

$$S_r = 100\% \times \left|\frac{1}{Q}\frac{\partial Q}{\partial T}\right| \text{ in } [\%\ 1/°C],$$

where Q is either τ_r or t_m. The quantity S_a represents the change in sensor value per unit change in temperature, while S_r is essentially the normalized absolute sensor sensitivity with respect to the chosen metric. Absolute sensitivities are constant, with values of 0.66 μs °C^{-1} for the rise time, and 1.29 μs °C^{-1} for the time-to-max. The maximal value of the relative sensitivity of rise-time based thermometry then reaches 5.53 %°C^{-1} at 200°C and is among the highest ever reported for luminescence thermometry (for a comparison please refer to the systematic list of luminescent-thermometer sensitivities given in Ref. 7). For time-to-max based thermometry, the relative sensitivity is 0.64 %°C^{-1}, which is still a high value compared to those reported previously.[7] It should also be noted that time-to-max parameters can be determined from measurements much more easily than rise times or decay times.

Conclusions

To conclude, with a suitable choice of rare-earth-doped materials, luminescence thermometry via emission rise times is a highly sensitive method for self-referenced temperature measurement. This method overcomes the deficiencies of decay time measurements, in terms of dynamic range and sensitivity, and imparts simplified data processing through the easy detection of emission intensity maxima (time-to-max parameter). In addition, a combined rise-time–decay-time analysis can be done from a single measurement. In the present case, the energy transfer between Eu^{3+} ions located in two adjacent sites of SrY_2O_4 facilitated an emission build-up with a notable rise time. In the 0.5 at.% doped sample, the rise-time value is temperature-quenched from 138 μs (at room temperature) to 13 μs (at 200°C). If needed, the dynamic range of measurement with this material can easily be extended, since the temporal dependence of emission is measurable well below microseconds. The shorter decay and rise times can be expected when this material is prepared in the form of small nanoparticles dispersed in an aqueous environment for the purpose of investigation of biological systems. Again, sufficient temporal resolution of measurement should be achievable, however, the applicability of the method in aqueous environment needs further investigation.

Acknowledgements

This work is supported by the Ministry of Education, Science and Technological Development of the Republic of Serbia (grant No. 45020) and the APV Provincial Secretariat for Science and Technological Development of the Republic of Serbia, through project no. 114-451-4787.

Notes and references

University of Belgrade, Vinča Institute of Nuclear Sciences, P.O. Box 522, 11001 Belgrade, Serbia
* Corresponding author E-mail: dramican@vinca.rs

1 X. D. Wang, O. S. Wolfbeis and R. J. Meier, *Chem. Soc. Rev.*, 2013, **42**, 7834.
2 P. R. N. Childs, J. R. Greenwood and C. A. Long, *Rev. Sci. Instrum.*, 2000, **71**, 2959.
3 V. M. Lojpur, G. Nikolić and M. D. Dramićanin, *J. Appl. Phys.*, 2014, **115**, 203106.
4 P. R. N. Childs, J. R. Greenwood and C. A. Long, *Rev. Sci. Instrum.*, 2000, **71**, 2959.
5 J. Lee and N. A. Kotov, *Nano Today*, 2007 **2**, 48.
6 Y. Yue and X. Wang, *Nano Reviews*, 2012, **3**, 11586.
7 C. D. S. Brites, P. P. Lima, N. J. O. Silva, A. Millan, V. S. Amaral, F. Palacio and L. D. Carlos, *Nanoscale*, 2012, **4**, 4799.
8 D. Jaque and F. Vetrone, *Nanoscale*, 2012, **4**, 4301.
9 L. H. Fisher, G. S. Harms and O. S. Wolfbeis, *Angew. Chem. Int.*, 2011, **50**, 4546.
10 A. Khalid and K. Kontis, *Sensors*, 2008, **8**, 5673.
11 V. Lojpur, M. G. Nikolić, D. Jovanović, M. Medić, Ž. Antić and M. D. Dramićanin, *Appl. Phys. Lett.*, 2013, **103**, 141912.
12 L. Liu, S. Creten, Y. Firdaus, J. J. A. F. Cuautle, M. Kouyaté, M. Van der Auweraer and C. Glorieux, *Appl. Phys. Lett.*, 2014, **104**, 031902.
13 L. M. Maestro, P. Haro-Gonzalez, J. G. Coello and D. Jaque, *Appl. Phys. Lett.*, 2012, **100**, 201110.
14 B. Dong, R. N. Hua, B. S. Cao, Z. P. Li, Y. Y. He, Z. Y. Zhang and O. S. Wolfbeis, *Phys. Chem. Chem. Phys.*, 2014, **16**, 20009.
15 V. A. Vlaskin, N. Janssen, J. Rijssel, R. Beaulac and D. R. Gammelin, *Nano Lett.*, 2010, **10**, 3670.
16 L. M. Maestro, E. M. Rodríguez, F. S. Rodríguez, I. M. C. Cruz, A. Juarranz, R. Naccache, F. Vetrone, D. Jaque, J. A. Capobianco and J. G. Solé, *Nano Lett.*, 2010, **10**, 5109.

17 M. G. Nikolić, Ž. Antić, S. Ćulubrk, J. M. Nedeljković and M. D. Dramićanin, *Sens. Actuators, B*, 2014, **201**, 46.
18 T. Gavrilović, D. Jovanović, V. Lojpur and M. D. Dramićanin, *Sci. Rep*., 2014, **4**, 4209.
19 V. K. Rai and C. B. de Araujo, *Spectrochim. Acta, Part A*, 2008, **71**, 116.
20 V. K. Rai and S. B. Rai, *Appl. Phys. B*, 2007, **87**, 323.
21 R. M. Ranson, E. Evangelou and C. B. Thomas, *Appl. Phys. Lett*., 1998, **72**, 2663.
22 S. W. Allison, S. M. Goedeke, M. R. Cates, W. A. Hollerman, J. I. Eldridge and T. J. Bencic, *Fluorescence Rise time Measurements for High Temperature Fluorescence-Based Thermometry*, Oak Ridge National Laboratories Report USDOE 2005 R05-12305.
23 J. Heber, K. H. Hellewege, V. Kobler and H. Murmann, *Zeitschrift für Physik*, 1970, **114**, 237.
24 X. M. Liu, C. K. Lin, Y. Luo and J. Lin, *J. Electrochem. Soc*., 2007, **154**, 21.
25 R. C. Ropp, in *Encyclopedia of the Alkaline Earth Compounds*, Elsevier, Amsterdam, 1st edn,, 2012, ch. 7, p. 649.
26 E. Pavitra, G. S. R. Raju, W. Park and J. S. Yu, *New J. Chem*., 2014, **38**, 163.
27 Z. Fu, S. Zhou, Y. Yu and S. Zhang, *J. Phys. Chem. B*, 2005, **109**, 23320.
28 R. Atkins and A. L. Diaz, *J. Lumin.*, 2008, **128**, 1463.
29 Y. Zhang, D. Geng, M. Shang, X. Zhang, X. Li, Z. Cheng, H. Lian and J. Lin, *Dalton Trans*., 2013, **42**, 4799.
30 E. Pavitra, G. S. R. Raju, Y. H. Ko and J. S. Yu, *Phys. Chem. Chem. Phys*., 2012, **14**, 11296.
31 R. B. Hunt, Jr. and R. G. Pappalardo, *J. Lumin*., 1985, **34**, 133.
32 A. H. Khalid and K. Kontis, *Meas. Sci. Technol*., 2009, **20**, 025305.

